Frontiers of Physics
https://doi.org/10.1007/s11467-021-1130-5
Front. Phys.
17(3), 31503 (2022)

RESEARCH ARTICLE

Highly efficient charging and discharging of three-level quantum batteries through shortcuts to adiabaticity

Fu-Quan Dou†, Yuan-Jin Wang, Jian-An Sun

College of Physics and Electronic Engineering, Northwest Normal University, Lanzhou 730070, China
Corresponding author. E-mail: †doufq@nwnu.edu.cn
Received September 1, 2021; accepted October 8, 2021

Quantum batteries are energy storage devices that satisfy quantum mechanical principles. How to improve the battery's performance such as stored energy and power is a crucial element in the quantum battery. Here, we investigate the charging and discharging dynamics of a three-level counterdiabatic stimulated Raman adiabatic passage quantum battery via shortcuts to adiabaticity, which can compensate for undesired transitions to realize a fast adiabatic evolution through the application of an additional control field to an initial Hamiltonian. The scheme can significantly speed up the charging and discharging processes of a three-level quantum battery and obtain more stored energy and higher power compared with the original stimulated Raman adiabatic passage. We explore the effect of both the amplitude and the delay time of driving fields on the performances of the quantum battery. Possible experimental implementation in superconducting circuit and nitrogen–vacancy center is also discussed.

Keywords quantum battery, charging and discharging dynamics, shortcuts to adiabaticity

1 Introduction

Quantum batteries are quantum mechanical systems which are able to store or release energy and satisfy the requirement of miniature battery [1, 2]. Currently widely used batteries are electrochemical devices [3] that store energy into chemical energy and convert it into electrical energy to drive machines to work. As many electronic devices continue to be miniaturized to provide flexibility and portability [4] and quantum technologies continue to make progress, it has become a prevalent topic to construct completely new energy storage devices called quantum batteries. They are based on quantum thermodynamics, which are fundamentally different from and transcend the traditional electrochemical batteries [3]. The influences of quantum phenomena [5–13] such as coherence and entanglement on quantum batteries must be taken into account.

Since the introduction of quantum batteries in 2013 [14], quantum phenomena have been used to improve the performances of the quantum batteries in various models [15, 16], such as quantum cavity [9, 17–25], spin chain [26–32], Sachdev–Ye–Kitaev model [33, 34], and quantum oscillators [35–38], showing quantum advantages. In the quantum cavity, a Dicke quantum battery is constructed by coupling N two-level systems with a single photonic mode in a cavity [18]. Interestingly, this collective charging protocol increases the charging power of a quantum battery by $\sqrt{N}$ times than the parallel one that assigns a single optical cavity to each two-level system [17]. In fact, this collective quantum advantage that enhances the charging power of quantum batteries is widespread [12]. Moreover, the charging power of a many-body quantum battery is further enhanced by considering the spin–spin interaction in the spin chain [26]. The exactly solvable Sachdev–Ye–Kitaev model is also a suitable cell for describing quantum batteries, which has shown that the presence of non-local correlations can significantly inhibit the fluctuations of the average energy stored in quantum batteries [34]. The quantum battery in quantum oscillators model consists of N two-level atoms, and is charged through a harmonic charging field, which is significantly different from a static charging field. In the absence of interatomic interaction, it can be fully charged by appropriately adjusting driving frequency. The fully charging power can be further enhanced when repulsive interaction exists between large N atoms [35].

Recently, based on stimulated Raman adiabatic passage (STIRAP) technique, one propose a three-level quantum battery [39, 40], which is a three-level system driven by two external optical or microwave fields that realizes the energy transfer between the ground state and the maxi-

* arXiv: 2104.13668. This article can also be found at http://journal.hep.com.cn/fop/EN/10.1007/s11467-021-1130-5.

© Higher Education Press 2022

mum excited state along the so-called dark state [41–43]. The characteristics of three-level systems that base on STIRAP to achieve quantum transitions have been studied in detail. For example, the loss due to spontaneous emission of the intermediate state is negligible, and the process is relatively insensitive to experimental imperfections in pulse intensity, shape and timing [43]. These characteristics suppress undesired spontaneous discharging, and greatly enhance the stability and robustness of a three-level quantum battery charged by STIRAP [39]. On that basis, it is shown that when an appropriate third driving field is applied to STIRAP, the transitions between the three quantum states can form a closed loop, which can effectively improve the charging power of the quantum battery [40]. However, in order to maintain the system as closely as possible in the dark state, in general, it requires rather long time to satisfy adiabaticity.

The protocol of shortcuts to adiabaticity (STA) [44, 45] is capable of accelerating the evolution in STIRAP and can be achieved by implementing an auxiliary field to suppress the nonadiabatic excitation in STIRAP. This method is also named counterdiabatic, transitionless or superadiabatic driving [46–51]. It has been widely used in atomic, molecular, optical and other fields [45, 52, 53]. Experimentally, it has been implemented in superconducting circuit [54], nitrogen–vacancy (N–V) centre [55–57], cold atoms [58, 59], etc. Very recently, the transitionless driven quantum batteries, composed by a set of independent three-qubit cells are proposed and the energy resources can be further optimized by implementing the transitionless technique [60].

In this paper, we investigate the characteristics of a three-level quantum battery when it is charged and discharged through STA. More specifically, based on counterdiabatic driving, we require an additional control field to ensure adiabaticity and form a three-level counterdiabatic STIRAP (cdSTIRAP) quantum battery. We are primarily concerned with the ergotropy which is the maximal energy can be extracted from the quantum battery to perform thermodynamic work [24, 61–65] and power of the quantum battery. We consider that the counterdiabatic protocol will enhance the charging and discharging power. To prove it, we study the properties of the cdSTIRAP quantum battery and compare them with STIRAP case. Meanwhile, we also simulate the effects of the amplitude and the delay time of driving fields on the charging process. Finally, we discuss the feasible schemes of our cdSTIRAP quantum battery in experiments.

The paper is organized as follows. In Section 2, we show a three-level quantum battery and charging (discharging) protocols. The Hamiltonian of the quantum battery involved in the corresponding protocol is introduced. Next in Section 3, we analyze the characteristics of the two charging protocols and calculated the corresponding maximum charging energy and average power. Then, the discharging processes are analyzed through STA in Section 4. We explore the feasible schemes of our cdSTIRAP quantum batteries in experiments in Section 5. Finally, a brief summary and discussion are reported in Section 6.

2 Model

In this section, we first briefly introduce the three-level quantum battery. The quantum battery Hamiltonian is $H_0 = \Sigma_{i=1}^{3}\varepsilon_i \left|i\right\rangle \left\langle i\right|$. Here $\left|i\right\rangle$ are the energy eigenstate of a three-level system, and ε_i stand for the corresponding eigenenergies. The ground state $\left|1\right\rangle$ denotes a discharged battery. When the system is in the first excited state $\left|2\right\rangle$, it is similar to a partially charged quantum battery. And the system requires to be in the second excited state $\left|3\right\rangle$ when the quantum battery is fully charged (see Fig. 1).

As shown in Fig. 1(a), the STIRAP charging or discharging protocol involves a P pulse on $\left|1\right\rangle$–$\left|2\right\rangle$ transition and a S pulse on $\left|2\right\rangle$–$\left|3\right\rangle$ transition. And the charging or discharging Hamiltonian under a time-dependent interaction picture reads [39, 52, 55]

$$H_1 = \frac{\hbar}{2}\begin{pmatrix} 0 & \Omega_p(t) & 0 \\ \Omega_p(t) & 0 & \Omega_s(t) \\ 0 & \Omega_s(t) & 0 \end{pmatrix}, \tag{1}$$

where $\hbar$ is the reduced Planck constant ($\hbar = 1$), and $\Omega_p(t)$, $\Omega_s(t)$ represent the amplitudes of the corresponding driving fields.

The three instantaneous eigenstates of Hamiltonian (1)

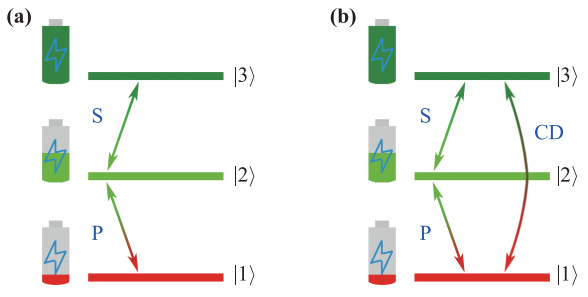

Fig. 1 Three-level quantum battery configuration and charging (discharging) schemes. **(a)** STIRAP charging (discharging) protocol. The ground state $\left|1\right\rangle$, the first excited state $\left|2\right\rangle$ and the second excited $\left|3\right\rangle$ are colored red, light green and dark green respectively, representing the bare (discharged) battery, partially charged battery and fully charged battery in turn. The charging of the quantum battery is realized by the transitions between quantum states. We utilize P pulse to drive $\left|1\right\rangle$–$\left|2\right\rangle$ transition and S pulse to realize $\left|2\right\rangle$–$\left|3\right\rangle$ transition. **(b)** cdSTIRAP charging (discharging) protocol. On the basis of (a), to compensate for nonadiabatic transitions, applying additional field CD to control $\left|1\right\rangle$–$\left|3\right\rangle$ transition.

are

$$|-\rangle = \frac{\sin\theta|1\rangle - |2\rangle + \cos\theta|3\rangle}{\sqrt{2}},$$
$$|0\rangle = \cos\theta|1\rangle - \sin\theta|3\rangle, \tag{2}$$
$$|+\rangle = \frac{\sin\theta|1\rangle + |2\rangle + \cos\theta|3\rangle}{\sqrt{2}},$$

and the corresponding eigenvalues are $\lambda_- = -\Omega(t)/2, \lambda_0 = 0, \lambda_+ = \Omega(t)/2$, respectively. Here $\Omega(t) = \sqrt{\Omega_p^2(t) + \Omega_s^2(t)}$, and $\tan\theta(t) = \Omega_p(t)/\Omega_s(t)$. The intermediate state $|0\rangle$ is called the dark state, which connects the $|1\rangle$ and $|3\rangle$ states without need of state $|2\rangle$. Maintaining the alignment of the state vector with the dark state (i.e., adiabatic following) is a basic feature of the STIRAP process. This requires that the adiabatic condition must be satisfied in the standard STIRAP [41, 66].

Figure 1(b) shows the cdSTIRAP protocol. The only difference from STIRAP protocol is that an additional driving field CD is applied to compensate for the nonadiabatic excitation. Thus, the complete interaction Hamiltonian becomes

$$H_2 = H_1 + H_{cd}, \tag{3}$$

with

$$H_{cd} = \frac{1}{2}\begin{pmatrix} 0 & 0 & \Omega_{cd}(t)\mathrm{e}^{\mathrm{i}\phi} \\ 0 & 0 & 0 \\ \Omega_{cd}(t)\mathrm{e}^{-\mathrm{i}\phi} & 0 & 0 \end{pmatrix}. \tag{4}$$

Here $\Omega_{cd}(t)$ is the amplitude of the CD field and the phase $\phi = \pi/2$.

For the purpose to obtain exact magnitude of $\Omega_{cd}(t)$ and maintain the adiabatic evolution of the system, we convert the Hamiltonian H_2 into a new matrix with three eigenstates in (2) as the base vector. The transformation matrix [52] is

$$U = \begin{pmatrix} \frac{\sin\theta}{\sqrt{2}} & -\frac{1}{\sqrt{2}} & \frac{\cos\theta}{\sqrt{2}} \\ \cos\theta & 0 & -\sin\theta \\ \frac{\sin\theta}{\sqrt{2}} & \frac{1}{\sqrt{2}} & \frac{\cos\theta}{\sqrt{2}} \end{pmatrix}. \tag{5}$$

Then, we make use of $H_2^{'}$ to represent the new matrix, which satisfies

$$H_2^{'} = UH_2U^{-1} + \mathrm{i}\frac{\mathrm{d}U}{\mathrm{d}t}U^{-1}. \tag{6}$$

Apparently,

$$H_2^{'} = \begin{pmatrix} -\frac{1}{2}\Omega(t) & \frac{\mathrm{i}}{\sqrt{2}}\left(\dot{\theta} - \frac{\Omega_{cd}(t)}{2}\right) & 0 \\ \frac{-\mathrm{i}}{\sqrt{2}}\left(\dot{\theta} - \frac{\Omega_{cd}(t)}{2}\right) & 0 & \frac{-\mathrm{i}}{\sqrt{2}}\left(\dot{\theta} - \frac{\Omega_{cd}(t)}{2}\right) \\ 0 & \frac{\mathrm{i}}{\sqrt{2}}\left(\dot{\theta} - \frac{\Omega_{cd}(t)}{2}\right) & \frac{1}{2}\Omega(t) \end{pmatrix}. \tag{7}$$

Note that when we take

$$\Omega_{cd}(t) = 2\dot{\theta}(t), \tag{8}$$

the off-diagonal elements in $H_2^{'}$ will vanish [52, 54, 67]. It means that the system will be locked in the dark state during adiabatic evolution, i.e., the three-level quantum battery can be charged or discharge through STA.

Consistent with Refs. [39, 40], we define the battery energy at time t is $E(t) = Tr\{H_0\rho(t)\}$, where $\rho(t)$ is the density matrix.

During charging, the ergotropy in quantum battery is

$$C(t) = E(t) - \varepsilon_1. \tag{9}$$

The charging power defines

$$P(t) = \frac{C(t)}{t_c}, \tag{10}$$

while the discharging ergotropy is

$$C(t) = \varepsilon_3 - E(t), \tag{11}$$

and the discharging power is

$$P_d(t) = \frac{C(t)}{t_d}, \tag{12}$$

where t_c and t_d are the charging and discharging time, respectively.

3 Charging dynamics

We now study the charging characteristics of quantum battery via cdSTIRAP protocol. In following analyses, we consider the driving fields are Gaussian pulses, of the form

$$\Omega_p(t) = \Omega_0\mathrm{e}^{-\left(\frac{t-\tau}{T}\right)^2}, \Omega_s(t) = \Omega_0\mathrm{e}^{-\left(\frac{t+\tau}{T}\right)^2}, \tag{13}$$

with delay τ, peak value Ω_0 and width T. The additional driving field CD is realized by modulating

$$\Omega_{cd}(t) = \frac{4\tau}{T^2}\mathrm{sech}\left(\frac{4\tau}{T^2}t\right). \tag{14}$$

In all following calculations, for simplicity, we choose the energy spectrum of the three-level system as $\varepsilon_1 = 0, \varepsilon_2 = 1$ and $\varepsilon_3 = 1.95$. The stable charging strategy for our quantum battery is through the eigenstate $|0\rangle$. Therefore the ergotropy is then

$$C(t) = \varepsilon_3\sin^2\theta + \varepsilon_1\cos^2\theta - \varepsilon_1$$
$$= 1.95\left[\frac{\Omega_p(t)}{\Omega(t)}\right]^2 = \frac{1.95}{1 + \mathrm{e}^{-\frac{4\tau t}{T}}}. \tag{15}$$

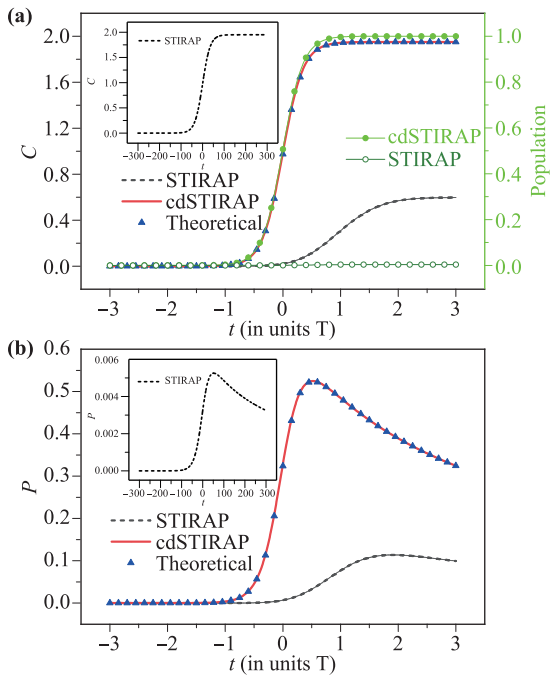

Fig. 2 Time evolution of ergotropy, population of the second excited state **(a)** and power **(b)** during charging. The red solid line and black dashed line correspond to cdSTIRAP and STIRAP charging protocol, respectively. The blue triangles represent the analytical solution of Eq. (15). The blue solid circle and olive hollow circle stand for the population of the second excited state for cdSTIRAP and STIRAP, respectively. The parameters selected for these data are width $T = 1$, peak value $\Omega_0 = 1$, and delay $\tau = 0.7T$. (Inset) Same as in the main panel but for $T = 100$, representing standard STIRAP charging protocol. We chose the energy spectrum of the three-level system as $\varepsilon_1 = 0, \varepsilon_2 = 1$ and $\varepsilon_3 = 1.95$.

We assume that the system is initially prepared in the ground state (corresponding to a discharged battery). Figure 2 shows the variation characteristics of ergotropy, population of the second excited state and power over time under specific parameters. The red solid line indicates the adiabatic evolution in cdSTIRAP charging protocol. The blue triangles represent the analytical solution of Eq. (15). We find that the numerical results are in complete agreement with the analytical results of Eq. (15) for cdSTIRAP charging protocol. For comparison purposes, the STIRAP charging protocol is also depicted with a black dashed line under the same parameters. As shown in Fig. 2(a), due to the accelerating the evolution, the cdSTIRAP charging protocol realize the complete and stable charging of the quantum battery in a very short time. This can also be further demonstrated by the time evolution of the population. In Fig. 2(a), we show the time evolution of populations in the second excited state, which are represented by green solid circle and olive hollow circle for cdSTIRAP and STIRAP, respectively. The population can transfer quickly for cdSTIRAP, while it barely changes for STIRAP (only arrive to 3.75×10^{-3}) at the end time. During the entire charging process, the ergotropy stored through STIRAP charging protocol is less than half of the maximum stored ergotropy. What's more, it is interesting to find that the cdSTIRAP can significantly improve the charging power of the quantum battery in Fig. 2(b). At the initial moment, the difference between the charging power of the two cases can be neglected. With the increase of time, the advantage of counterdiabatic driving gradually appears. The charging power gradually reaches its maximum value at some point of time. Then, the two charging powers slowly drop as time goes on. During which the charging power of cdSTIRAP charging protocol always greater than the STIRAP one. It is worth attentioning that the maximum charging power increased more than four times. In the insets of Fig. 2, we display the charging process in the standard STIRAP protocol. Obviously, to achieve the adiabatic evolution of the quantum state and make the quantum battery fully charged, one has to increase the charging time to satisfy the adiabatic condition. As a result, the charging power is greatly reduced, the maximum value only 1% of the cdSTIRAP protocol.

The effect of delay τ and peak value Ω_0 on maximum ergotropy and charging power is shown in Fig. 3. Figures 3(a) and (c) illustrate the dependencies of the maximum ergotropy and maximum charging power on delay time τ. It is noteworthy that the two charging protocols are identical when the value of τ is taken as 0 (corresponding to $\Omega_{cd} = 0$). Once the delay τ sets in, the two protocols immediately deviate from each other; the maximum ergotropy and charging power in the cdSTIRAP increase and the maximum ergotropy can approach and hold in the maximum value as τ increases [see also Eq. (15)], whereas those in the STIRAP decrease. Figures 3(b) and

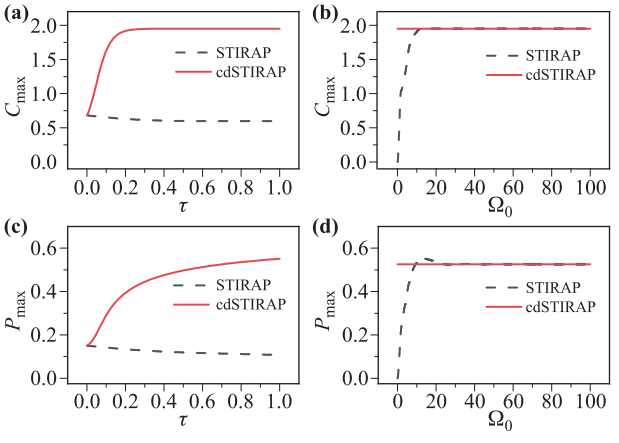

Fig. 3 The maximum ergotropy $C_{\max}$ as a function of **(a)** τ and **(b)** peak value Ω_0. The dependence of the maximum charging power $P_{\max}$ on **(c)** τ and **(d)** Ω_0. For all figures, the parameter T is set to 1, and color coding, labeling and other parameters are the same as in Fig. 2.

(d) show the maximum ergotropy and charging power as functions of Ω_0. The cdSTIRAP charging protocol shows good stability; for different Ω_0 it can always make the quantum battery fully charged. Interestingly, the maximum charging power is not influenced by Ω_0. This is due to the fact that the charging ergotropy is independent to the peak value Ω_0 [see Eq. (15)] and $\Omega_0 = 0$ corresponds to the case of the resonant π pulse (see also Appendix). The advantages of the cdSTIRAP protocol are quite obvious. Especially when the Ω_0 is relatively small, the maximum ergotropy and charging power far exceed the STIRAP charging protocol.

4 Discharging character

The discharging process of the quantum battery can also be realized through STA. We assume that a quantum battery is already fully charged, i.e., the three-level system is on the second excited state, and the energy is extracted by transitioning it back to the ground state. Similarly, the STA is able to accelerate this discharging process.

In STIRAP discharging protocol, energy is released by changing the sequence of pulses. More specifically, the STIRAP discharging protocol exploits a first P pulse on $|1\rangle$–$|2\rangle$ transition and a second S pulse on $|2\rangle$–$|3\rangle$ transition. That means they take the form

$$\Omega_p(t) = \Omega_0 \mathrm{e}^{-\left(\frac{t+\tau}{T}\right)^2}, \quad \Omega_s(t) = \Omega_0 \mathrm{e}^{-\left(\frac{t-\tau}{T}\right)^2}. \tag{16}$$

As for cdSTIRAP discharging protocol, to ensure the quantum battery discharge through STA, a counterdiabatic pulse is added on this basis, which satisfies

$$\Omega_{cd}(t) = -\frac{4\tau}{T^2}\mathrm{sech}\left(\frac{4\tau}{T^2}t\right). \tag{17}$$

Similarity, the corresponding discharging ergotropy is

$$\begin{aligned} C(t) &= \varepsilon_3 - (\varepsilon_3 \sin^2\theta + \varepsilon_1 \cos^2\theta) \\ &= 1.95\left[\frac{\Omega_s(t)}{\Omega(t)}\right]^2 = \frac{1.95}{1+\mathrm{e}^{\frac{4\tau t}{T}}}. \end{aligned} \tag{18}$$

Figure 4 presents the time evolution of ergotropy, population of the second excited state and power in two different discharging protocols. The blue triangles represent the analytical solution of Eq. (18). Clearly, the numerical results are in complete agreement with the analytical results of Eq. (18) for cdSTIRAP protocol. The STIRAP discharge protocol at most can only extract part of the energy stored in the quantum battery. In contrast, the cdSTIRAP discharge protocol can not only make full use of all the energy in the quantum battery, but also obviously release the energy faster [Fig. 4(a)]. This power advantage is also illustrated in Fig. 4(b), which is more suitable for some high-power appliances.

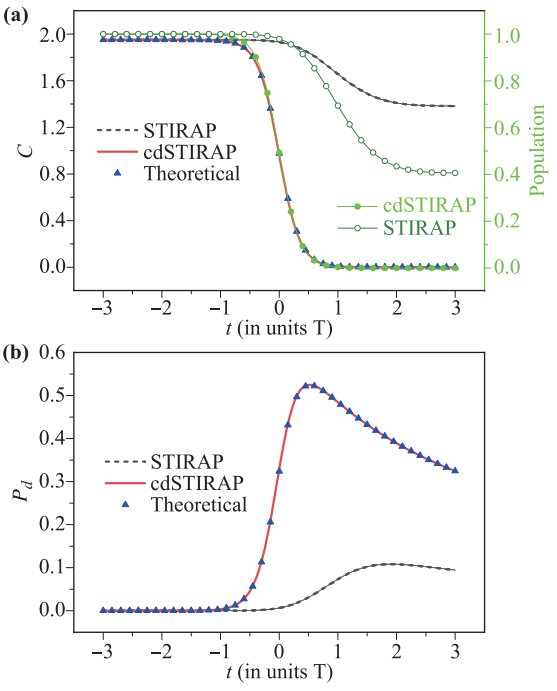

Fig. 4 Time evolution of ergotropy, population of the second excited state **(a)** and power **(b)** during discharging. The analytical solution is given by Eq. (18). Color coding, labeling and parameters are the same as in Fig. 2.

5 Implement

The cdSTIRAP charging and discharging protocols described here can be implemented in different physical systems driven by optical excitations or microwave excitations, like superconducting circuit and N–V centre. Supposing we use circuit quantum electrodynamics as the experimental platform [54, 68], the first three states of a superconducting transmon circuit constitute a three-level quantum battery. Two microwave pulses are used to realize STIRAP, and an additional two-photon microwave pulse is needed to suppress nonadiabatic excitations and thereby realize cdSTIRAP. Encouragingly, just recently, an experimental realization of a three-level quantum battery based on superconducting qubits has been reported and the stable and powerful charging processes by exploring dark and bright states have also been achieved, respectively [69]. The negatively charged N–V centre in the diamond lattice is also an excellent experimental platform [55, 56]. It has a $S = 1$ spin system which is equivalent to a three-level quantum battery in its orbital ground state. The N–V's spin sublevels are $|0\rangle$ and $|\pm 1\rangle$. It can achieve STIRAP charging or discharging protocol by driving the $|0\rangle \leftrightarrow |\pm 1\rangle$ transitions with microwave magnetic fields. In addition, applying a time-varying strain field to control the $|-1\rangle \leftrightarrow |+1\rangle$ transition, which compensate for nonadiabatic transitions and implement the cdSTIRAP.

6 Conclusion and discussion

In conclusion, we have introduced the concept of a cdSTIRAP quantum battery, a three-level quantum system charged or discharged through STIRAP and STA based on counterdiabatic driving to accelerate charging or discharging processes. By calculation of the ergotropy and power variation over time, we have confirmed the significant acceleration effect of STA on the charging and discharging process of quantum battery. The maximum charge energy can be increased approximately 3 to 4 times, while the maximum charge power can be increased 4 to 5 times. In addition, we have also studied the impact of different delay τ and peak value Ω_0 on the quantum battery. We found that the performance of a cdSTIRAP quantum battery not vary with peak value, but raising the value of delay time would lead to a larger maximum charging power. We finally proposed that superconducting circuit or N–V centre provide a promising implementation for our cdSTIRAP quantum batteries. This study aims to provide a more efficient three-level quantum battery theoretical background in view of future experimental implementations.

It is should be pointed out that (i) the present cdSTIRAP quantum batteries must employ a specific time-dependent additional field pulse Ω_{cd}; (ii) the additional field formes a closed interaction loop, which makes population transfer sensitive to the phases of the fields [41]. These constraints render that the procedure would be impractical. One natural question is: If it is possible to perform a resonant π laser pulse in the $|1\rangle$–$|3\rangle$ transition, then this pulse will produce the desired population transfer without the need of the S and P pulses [41]. In fact, if one is able to directly couple $|1\rangle$ to $|3\rangle$, the π pulse alone can transfer the population from $|1\rangle$ to $|3\rangle$ regardless of the pulse shape, i.e., no matter what kind of π pulse, the maximin energy of quantum battery can be reached. However, the battery power varies with the π pulse shape (see Appendix A). On the one hand, the π pulse is sensitive to pulse duration and peak amplitude. In addition, the use of the present cdSTIRAP scheme (which depends on at least two coherent pulses), rather than a single pulse coupling two states, offers many advantages: i) The transition efficiency can be made relatively insensitive to many of the experimental details of the pulses; ii) With the three-state system, one can produce transition between states for which the single-photon transitions are forbidden. Especially, it can be used to transfer population between magnetic sublevels or fine-structure levels [42]; iii) It is much more efficient due to accelerating the adiabatic transition precess by using the third additional field pulse. Furthermore, in our quantum battery model, the detuning and the middle-state decay are not considered. When these factors are taken into account, high efficient quantum battery can still be achieved via non-Hermitian STA, but with a more complex additional fields form [70]. After finishing this work, we became aware of a recent article [71], in which a similar STA method is employed to speed up the adiabatic charging process of quantum batteries. The main qualitative features of our results agree with those in Ref. [71] confirms the excellent performance of cdSTIRAP quantum batteries.

Acknowledgements The work was supported by the National Natural Science Foundation of China (Grant No. 12075193).

Appendix A cdSTIRAP versus π pulses

This appendix is contributed to compare cdSTIRAP with single resonance π pulses. We apply a resonant π laser pulse to the $|1\rangle$–$|3\rangle$ transition, then this pulse will produce the desired population transfer without the need of the S and P pulses. Thus, the quantum battery can also be achieved by a single resonance π pulse. Figure A1 and Fig. A2 display the charging and discharging energy and power for different π pulses, respectively. The black square represents the cdSTIRAP in Section 3 and Section 4. Here we take the following π pulses as examples:

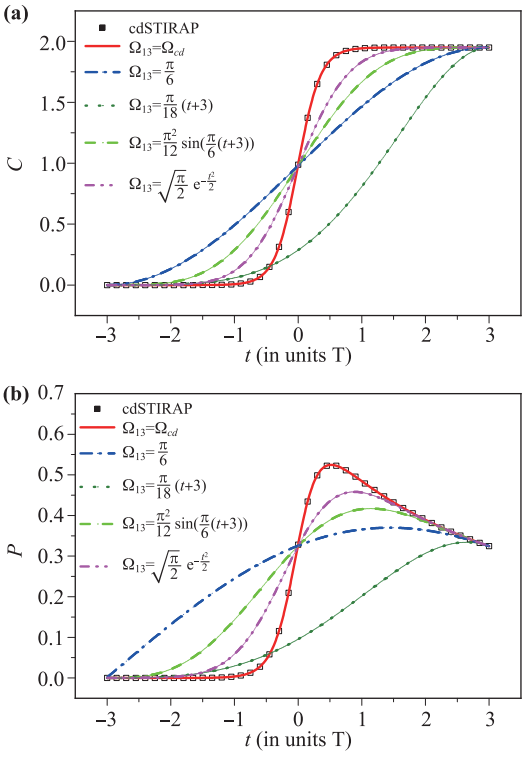

Fig. A1 Comparison of the time evolution of charging energy **(a)** and power **(b)** for different π pulses and cdSTIRAP protocol. The balck squares represent the cdSTIRAP in Section 4. The parameter $T = 1$.

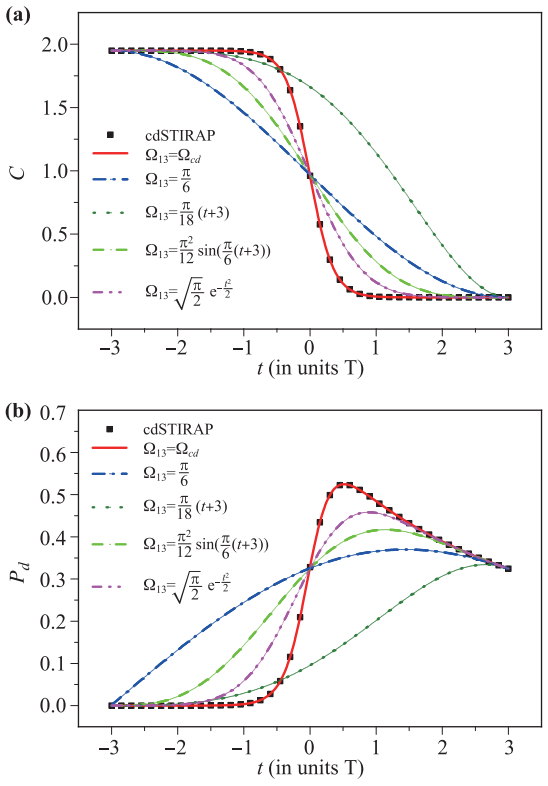

Fig. A2 Comparison of the time evolution of discharging energy **(a)** and power **(b)** for different π pulses and cdSTIRAP protocol. The balck squares represent the cdSTIRAP in Section 5. The parameter $T = 1$.

$\Omega_{13}(t) = \Omega_{cd}, \pi/6, \pi(t+3)/18, \frac{\pi^2}{12}\sin\frac{\pi(t+3)}{6}, \sqrt{\pi/2}e^{-\frac{t^2}{2}}$. The same as before, the evolution time $t = [-3T, 3T]$ and $T = 1$. The results show that all single π pulse can reach the maximum energy value of the quantum battery. However, the power is different for different pulse shape. In fact, in the quantum battery system, if only apply a resonant π laser pulse, the battery energy is

$$C(t) = \varepsilon_3 \sin^2\frac{A(t)}{2} = 1.95\sin^2\frac{A(t)}{2}, \tag{1}$$

where the pulse area $A(t) = \int_{-3T}^{t}\Omega_{13}(t)\mathrm{d}t$. Obviously, when $\Omega_{13} = \Omega_{cd}$, $A(t)/2 = \theta$. This is an issue worthy of further exploration: whether there is a more efficient resonant pulse to achieve a more optimized power when $|1\rangle$ and $|3\rangle$ can be directly coupled.

References

1. F. Campaioli, F. A. Pollock, and S. Vinjanampathy, Quantum batteries, in: Thermodynamics in the Quantum Regime: Fundamental Aspects and New Directions, edited by F. Binder, L. A. Correa, C. Gogolin, J. Anders, and G. Adesso, Springer International Publishing, Cham, 2018, pp 207–225
2. S. Bhattacharjee and A. Dutta, Quantum thermal machines and batteries, arXiv: 2008.07889 [quant-ph] (2020)
3. J. Q. Quach and W. J. Munro, Using dark states to charge and stabilise open quantum batteries, arXiv: 2002.10044 [quant-ph] (2020)
4. K. Sen and U. Sen, Local passivity and entanglement in shared quantum batteries, arXiv: 1911.05540 [quant-ph] (2019)
5. F. H. Kamin, F. T. Tabesh, S. Salimi, and A. C. Santos, Entanglement, coherence and charging process of quantum batteries, *Phys. Rev. E* 102, 052109 (2020)
6. L. P. García-Pintos, A. Hamma, and A. del Campo, Fluctuations in extractable work bound the charging power of quantum batteries, *Phys. Rev. Lett.* 125(4), 040601 (2020)
7. M. Carrega, A. Crescente, D. Ferraro, and M. Sassetti, Dissipative dynamics of an open quantum battery, *New J. Phys.* 22(8), 083085 (2020)
8. F. Barra, Dissipative charging of a quantum battery, *Phys. Rev. Lett.* 122(21), 210601 (2019)
9. F. Pirmoradian and K. Mølmer, Aging of a quantum battery, *Phys. Rev. A* 100(4), 043833 (2019)
10. K. V. Hovhannisyan, M. Perarnau-Llobet, M. Huber, and A. Acín, Entanglement generation is not necessary for optimal work extraction, *Phys. Rev. Lett.* 111(24), 240401 (2013)
11. F. T. Tabesh, F. H. Kamin, and S. Salimi, Environment-mediated charging process of quantum batteries, arXiv: 2005.12823 [quant-ph] (2020)
12. F. Campaioli, F. A. Pollock, F. C. Binder, L. Céleri, J. Goold, S. Vinjanampathy, and K. Modi, Enhancing the charging power of quantum batteries, *Phys. Rev. Lett.* 118(15), 150601 (2017)
13. S. Gherardini, F. Campaioli, F. Caruso, and F. C. Binder, Stabilizing open quantum batteries by sequential measurements, *Phys. Rev. Research* 2(1), 013095 (2020)
14. R. Alicki and M. Fannes, Entanglement boost for extractable work from ensembles of quantum batteries, *Phys. Rev. E* 87(4), 042123 (2013)
15. J. Monsel, M. Fellous-Asiani, B. Huard, and A. Auffèves, The energetic cost of work extraction, *Phys. Rev. Lett.* 124(13), 130601 (2020)
16. F. H. Kamin, F. T. Tabesh, S. Salimi, F. Kheirandish, and A. C. Santos, Non-Markovian effects on charging and self-discharging process of quantum batteries, *New J. Phys.* 22(8), 083007 (2020)
17. D. Ferraro, M. Campisi, G. M. Andolina, V. Pellegrini, and M. Polini, High-power collective charging of a solid-state quantum battery, *Phys. Rev. Lett.* 120(11), 117702 (2018)
18. X. Zhang and M. blaauboer, Enhanced energy transfer in a Dicke quantum battery, arXiv: 1812.10139 [quant-ph] (2018)
19. G. M. Andolina, M. Keck, A. Mari, M. Campisi, V. Giovannetti, and M. Polini, Extractable work, the role of correlations, and asymptotic freedom in quantum batteries, *Phys. Rev. Lett.* 122(4), 047702 (2019)

20. F. C. Binder, S. Vinjanampathy, K. Modi, and J. Goold, Quantacell: Powerful charging of quantum batteries, *New J. Phys.* 17(7), 075015 (2015)
21. A. Crescente, M. Carrega, M. Sassetti, and D. Ferraro, Charging and energy fluctuations of a driven quantum battery, *New J. Phys.* 22(6), 063057 (2020)
22. S. Julià-Farré, T. Salamon, A. Riera, M. N. Bera, and M. Lewenstein, Bounds on the capacity and power of quantum batteries, *Phys. Rev. Research* 2(2), 023113 (2020)
23. B. Mohan and A. K. Pati, Reverse quantum speed limit: How slow quantum battery can discharge? arXiv: 2006.14523 [quant-ph] (2020)
24. W. Niedenzu, V. Mukherjee, A. Ghosh, A. G. Kofman, and G. Kurizki, Quantum engine efficiency bound beyond the second law of thermodynamics, *Nat. Commun.* 9(1), 165 (2018)
25. F. Caravelli, G. Coulter-De Wit, L. P. García-Pintos, and A. Hamma, Random quantum batteries, *Phys. Rev. Research* 2(2), 023095 (2020)
26. T. P. Le, J. Levinsen, K. Modi, M. M. Parish, and F. A. Pollock, Spin-chain model of a many-body quantum battery, *Phys. Rev. A* 97(2), 022106 (2018)
27. S. Ghosh, T. Chanda, and A. Sen(De), Enhancement in the performance of a quantum battery by ordered and disordered interactions, *Phys. Rev. A* 101(3), 032115 (2020)
28. F. Zhao, F. Q. Dou, and Q. Zhao, Quantum battery of interacting spins with environmental noise, *Phys. Rev. A* 103(3), 033715 (2021)
29. D. Rossini, G. M. Andolina, and M. Polini, Many-body localized quantum batteries, *Phys. Rev. B* 100(11), 115142 (2019)
30. S. Zakavati, F. T. Tabesh, and S. Salimi, Bounds on charging power of open quantum batteries, arXiv: 2003.09814 [quant-ph] (2020)
31. S. Ghosh, T. Chanda, S. Mal, and A. S. De, Fast charging of quantum battery assisted by noise, arXiv: 2005.12859 [quant-ph] (2020)
32. A. C. Santos, A. Saguia, and M. S. Sarandy, Stable and charge-switchable quantum batteries, *Phys. Rev. E* 101(6), 062114 (2020)
33. D. Rossini, G. M. Andolina, D. Rosa, M. Carrega, and M. Polini, Quantum charging supremacy via Sachdevye–Kitaev batteries, arXiv: 1912.07234 [condmat.str-el] (2019)
34. D. Rosa, D. Rossini, G. M. Andolina, M. Polini, and M. Carrega, Ultra stable charging of fastest scrambling quantum batteries, arXiv: 1912.07247 [condmat.str-el] (2019)
35. Y. Y. Zhang, T. R. Yang, L. Fu, and X. Wang, Powerful harmonic charging in a quantum battery, *Phys. Rev. E* 99(5), 052106 (2019)
36. G. M. Andolina, D. Farina, A. Mari, V. Pellegrini, V. Giovannetti, and M. Polini, Charger-mediated energy transfer in exactly solvable models for quantum batteries, *Phys. Rev. B* 98(20), 205423 (2018)
37. G. M. Andolina, M. Keck, A. Mari, V. Giovannetti, and M. Polini, Quantum versus classical many-body batteries, *Phys. Rev. B* 99(20), 205437 (2019)
38. J. Chen, L. Zhan, L. Shao, X. Zhang, Y. Zhang, and X. Wang, Charging quantum batteries with a general harmonic driving field, *Ann. Phys.* 532(4), 1900487 (2020)
39. A. C. Santos, B. Çakmak, S. Campbell, and N. T. Zinner, Stable adiabatic quantum batteries, *Phys. Rev. E* 100(3), 032107 (2019)
40. F. Q. Dou, Y. J. Wang, and J. A. Sun, Closed-loop three-level charged quantum battery, *EPL (Europhysics Letters)* 131(4), 43001 (2020)
41. N. V. Vitanov, A. A. Rangelov, B. W. Shore, and K. Bergmann, Stimulated Raman adiabatic passage in physics, chemistry, and beyond, *Rev. Mod. Phys.* 89(1), 015006 (2017)
42. K. Bergmann, H. Theuer, and B. W. Shore, Coherent population transfer among quantum states of atoms and molecules, *Rev. Mod. Phys.* 70(3), 1003 (1998)
43. B. W. Shore, Picturing stimulated Raman adiabatic passage: A STIRAP tutorial, *Adv. Opt. Photonics* 9(3), 563 (2017)
44. X. Chen, I. Lizuain, A. Ruschhaupt, D. Guéry-Odelin, and J. G. Muga, Shortcut to adiabatic passage in two- and three-level atoms, *Phys. Rev. Lett.* 105(12), 123003 (2010)
45. D. Guéry-Odelin, A. Ruschhaupt, A. Kiely, E. Torrontegui, S. Martínez-Garaot, and J. G. Muga, Shortcuts to adiabaticity: Concepts, methods, and applications, *Rev. Mod. Phys.* 91(4), 045001 (2019)
46. M. Theisen, F. Petiziol, S. Carretta, P. Santini, and S. Wimberger, Superadiabatic driving of a three-level quantum system, *Phys. Rev. A* 96(1), 013431 (2017)
47. F. Dou, J. Liu, and L. Fu, High-fidelity superadiabatic population transfer of a two-level system with a linearly chirped Gaussian pulse, *EPL (Europhysics Letters)* 116(6), 60014 (2016)
48. M. V. Berry, Transitionless quantum driving, *J. Phys. A Math. Theor.* 42(36), 365303 (2009)
49. M. Demirplak and S. A. Rice, Adiabatic population transfer with control fields, *J. Phys. Chem. A* 107(46), 9937 (2003)
50. A. del Campo, Shortcuts to adiabaticity by counterdiabatic driving, *Phys. Rev. Lett.* 111(10), 100502 (2013)
51. L. Giannelli and E. Arimondo, Three-level superadiabatic quantum driving, *Phys. Rev. A* 89(3), 033419 (2014)
52. N. V. Vitanov and M. Drewsen, Highly efficient detection and separation of chiral molecules through shortcuts to adiabaticity, *Phys. Rev. Lett.* 122(17), 173202 (2019)
53. S. Li, P. Shen, T. Chen, and Z. Y. Xue, Noncyclic nonadiabatic holonomic quantum gates via shortcuts to adiabaticity, *Front. Phys.* 16(5), 51502 (2021)
54. A. Vepsäläinen, S. Danilin, and G. S. Paraoanu, Superadiabatic population transfer in a three-level superconducting circuit, *Sci. Adv.* 5(2), eaau5999 (2019)
55. A. Barfuss, J. Kölbl, L. Thiel, J. Teissier, M. Kasperczyk, and P. Maletinsky, Phase-controlled coherent dynamics of a single spin under closed-contour interaction, *Nat. Phys.* 14(11), 1087 (2018)

56. J. Kölbl, A. Barfuss, M. S. Kasperczyk, L. Thiel, A. A. Clerk, H. Ribeiro, and P. Maletinsky, Initialization of single spin dressed states using shortcuts to adiabaticity, *Phys. Rev. Lett.* 122(9), 090502 (2019)
57. J. Zhang, J. H. Shim, I. Niemeyer, T. Taniguchi, T. Teraji, H. Abe, S. Onoda, T. Yamamoto, T. Ohshima, J. Isoya, and D. Suter, Experimental implementation of assisted quantum adiabatic passage in a single spin, *Phys. Rev. Lett.* 110(24), 240501 (2013)
58. J. F. Schaff, X. L. Song, P. Capuzzi, P. Vignolo, and G. Labeyrie, Shortcut to adiabaticity for an interacting Bose–Einstein condensate, *EPL (Europhysics Letters)* 93(2), 23001 (2011)
59. Y. X. Du, Z. T. Liang, Y. C. Li, X. X. Yue, Q. X. Lv, W. Huang, X. Chen, H. Yan, and S. L. Zhu, Experimental realization of stimulated Raman shortcut-to-adiabatic passage with cold atoms, *Nat. Commun.* 7(1), 12479 (2016)
60. L. F. C. Moraes, A. Saguia, A. C. Santos, and M. S. Sarandy, Charging power and stability of always-on transitionless driven quantum batteries, arXiv: 2012.05855 [quant-ph] (2020)
61. A. E. Allahverdyan, R. Balian, and T. M. Nieuwenhuizen, Maximal work extraction from finite quantum systems, *EPL (Europhysics Letters)* 67(4), 565 (2004)
62. M. Alimuddin, T. Guha, and P. Parashar, Structure of passive states and its implication in charging quantum batteries, *Phys. Rev. E* 102(2), 022106 (2020)
63. B. Akmak, Ergotropy from coherences in an open quantum system, arXiv: 2005.08489 [quant-ph] (2020)
64. K. Ito and G. Watanabe, Collectively enhanced high-power and high-capacity charging of quantum batteries via quantum heat engines, arXiv: 2008.07089 [quant-ph] (2020)
65. F. Tacchino, T. F. F. Santos, D. Gerace, M. Campisi, and M. F. Santos, Non-equilibrium steady states as resources for quantum heat engines, arXiv: 2007.04463 [quant-ph] (2020)
66. J. R. Kuklinski, U. Gaubatz, F. T. Hioe, and K. Bergmann, Adiabatic population transfer in a three-level system driven by delayed laser pulses, *Phys. Rev. A* 40(11), 6741 (1989)
67. F. Petiziol, E. Arimondo, L. Giannelli, F. Mintert, and S. Wimberger, Optimized three-level quantum transfers based on frequency-modulated optical excitations, *Sci. Rep.* 10(1), 2185 (2020)
68. A. Vepsäläinen and G. S. Paraoanu, Simulating spin chains using a superconducting circuit: Gauge invariance, superadiabatic transport, and broken time-reversal symmetry, *Adv. Quantum Technol.* 3(4), 1900121 (2020)
69. C. K. Hu, J. Qiu, P. J. P. Souza, J. Yuan, Y. Zhou, L. Zhang, J. Chu, X. Pan, L. Hu, J. Li, Y. Xu, Y. Zhong, S. Liu, F. Yan, D. Tan, R. Bachelard, C. J. Villas-Boas, A. C. Santos, and D. Yu, Optimal charging of a superconducting quantum battery, arXiv: 2108.04298 [quant-ph] (2021)
70. J. H. Zhang and F. Q. Dou, High-fidelity formation of deeply bound ultracold molecules via non-Hermitian shortcut to adiabaticity, *New J. Phys.* 23(6), 063001 (2021)
71. H. Hu, S. Qi, and J. Jing, Fast and stable charging via a shortcut to adiabaticity, arXiv: 2104.12143 [quant-ph] (2021)